

Ultrafast Heating of Silicon on Sapphire by Femtosecond Optical Pulses

M. C. Downer^(a) and C. V. Shank

AT&T Bell Laboratories, Holmdel, New Jersey 07733

(Received 20 December 1985)

We monitor the refractive index $n + ik$ of an optically thin silicon layer following femtosecond photoexcitation below the threshold fluence E_{th} for melting, in order to measure the rate of lattice temperature rise. We find that most of the heating is delayed with respect to the photoexcitation, but becomes faster as E_{th} is approached. A model based on delayed Auger heating is presented.

PACS numbers: 79.20.Ds, 63.20.Kr, 78.65.Jd

The processes by which the energy of an intense short laser pulse is transferred to lattice heat in a solid upon absorption have been investigated extensively on the nanosecond and picosecond time scales.¹ Most of these experiments, even on the picosecond time scale, have supported the so-called optical heating model,² which assumes an instantaneous transfer of energy from the photoexcited electronic carrier system to the lattice. In the present work we use femtosecond optical pulses to resolve a delayed semiconductor lattice heating following photoexcitation.

Earlier experiments have used amplified femtosecond pulses to investigate the dynamics of melting and evaporation at a highly photoexcited silicon surface.³⁻⁵ These experiments have shown that a silicon surface becomes highly reflective^{3,5} and microscopically disordered⁴ in less than one picosecond following femtosecond pulsed excitation above a threshold fluence of approximately 0.1 J/cm^2 . The present experiment investigates the temperature rise of crystalline silicon excited below the threshold for melting, through time-resolved measurements of refractive index changes in a submicron silicon film. This technique, which has been used for nanosecond⁶ and picosecond⁷ time-resolved heating measurements, relies upon the well-characterized temperature dependence⁸ of the refractive index $n + ik$ of silicon in the wavelength range between the indirect (1.15 eV) and direct (3.0 eV) band gaps. The temperature dependence of the index results from a downward shift of the direct band edge of silicon caused by renormalization of the band energy by the electron-phonon interaction, with a small contribution from the lattice thermal expansion.⁹ Use of a thin film permits sensitive determination of small ($10^{-3} \Delta n/n < 10^{-2}$) heat-induced index changes through measurement of the optical interference fringes in the reflectance and transmittance spectra, and analysis using the thin-film optics equations.¹⁰

In our experiments optical pulses of 100 fs duration and approximately 0.3 mJ energy at 620 nm were provided by a colliding-pulse mode-locked ring dye laser¹¹ followed by a four-stage optical amplifier operating at a repetition rate of 10 Hz.¹² A beam splitter divided the

output beam into excitation and probe beams. The excitation beam was focused to a spot size of approximately $100 \mu\text{m}$ on the $0.5\text{-}\mu\text{m}$ -thick silicon film on a sapphire substrate, and attenuated to a fluence well below the damage threshold of 0.1 J/cm^2 to avoid sample damage by occasional intense pulses. The sample was rastered over a 2-mm-square area during data collection to guard against cumulative damage. The probe beam passed through a variable optical delay line, and was then focused into a cell containing water to generate a white-light continuum.¹³ The green-blue portion of this continuum beam was spectrally filtered and attenuated by a factor of 100 before being focused at near-normal incidence onto a spot overlapping the photoexcited area of the sample. In order to ensure that we studied a uniformly excited sample area, we selected probe light from a $10\text{-}\mu\text{m}$ -diam circular area near the center of the photoexcited region by imaging transmitted and reflected probe beams onto irises placed in the image planes.⁵ These spatially filtered beams, along with a reference probe beam, were then collected at the entrance slit of a spectrometer equipped with a vidicon detector. The normalized spectra between 480 and 580 nm were stored and analyzed with an optical multichannel analyzer.

Figure 1 shows (a) reflectivity and (b) transmission at time delays $\Delta t = -1, 0.5,$ and 200 ps following photoexcitation at a fluence of 0.02 J/cm^2 . In Fig. 1(a), the initial blue shift of the Fabry-Perot fringes at $\Delta t = 0.5 \text{ ps}$ results from a decrease in the real index n caused by the presence of a dense electron-hole plasma. The shift is more pronounced in the red, as expected from a Drude-model description of the plasma-induced index change. The slight decrease in fringe contrast results from a corresponding increase in the imaginary index k . At later time delays, the fringes drift back towards the red, passing the original positions in a few tens of picoseconds, before reaching a final red-shifted position evident in the curve at $\Delta t = 200 \text{ ps}$. Fringe contrast also recovers slightly. This red shift, which now is more pronounced in the blue, results from the lattice heating which accompanies the decay of the electron-hole plasma through Auger recombination. The corresponding transmis-

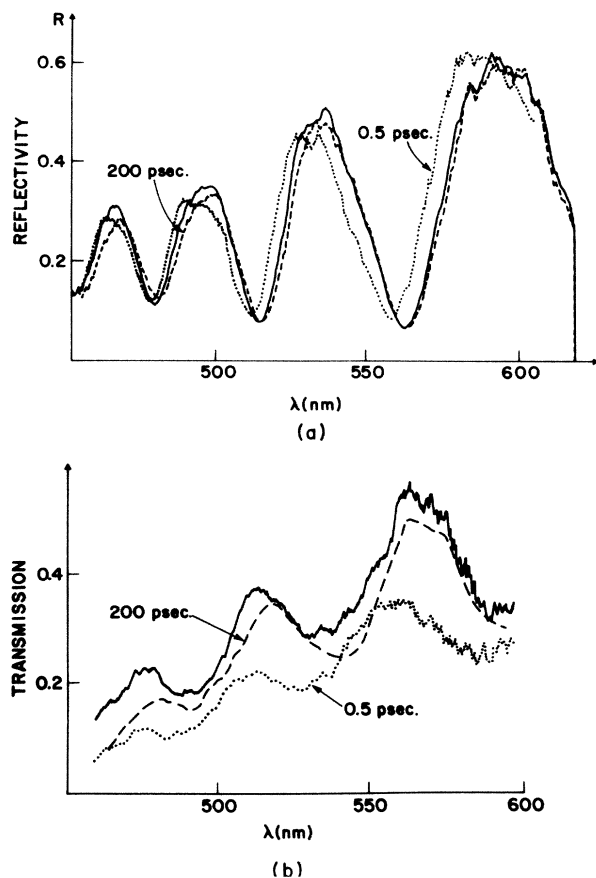


FIG. 1. Normalized experimental time-resolved (a) reflectivity and (b) transmission spectra of $0.5 \mu\text{m}$ silicon-on-sapphire film before excitation (solid curves), and 0.5 psec (dotted) and 200 psec (dashed) after excitation. Note strong Fabry-Perot interference fringes. In (a), note initial blue shift of fringes, caused by presence of dense electron-hole plasma, followed by red shift, caused by lattice heating. In (b), note strong initial photoinduced absorption, followed by partial recovery.

sion spectra in Fig. 1(b) show qualitatively similar shifts in fringe positions and contrast. The strong initial drop in transmission evident in the curve at $\Delta t = 0.5 \text{ ps}$, followed by a slow partial recovery, suggests that plasma-induced absorption, along with heating, contributed to the changes in k , as discussed more fully below.

We analyzed the data in Fig. 1 by extracting values of n and k from the reflectivity and transmission. A program was written which read the experimental R and T values for each wavelength and time delay, then solved the thin-film optics equations¹⁰ iteratively to find n and k values which yielded the experimental R and T within 0.2%. In this manner, we were able to confirm that our n and k values for the unexcited sample agreed with independent measurements.⁸ In addition, the temporal evolution of n and k could be stu-

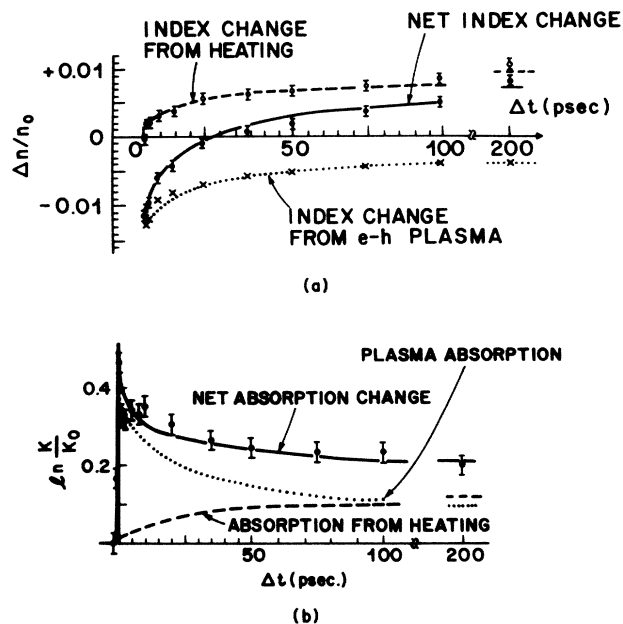


FIG. 2. Photoinduced fractional change in (a) real part of refractive index (n) and (b) imaginary refractive index (k) at 485 nm of an optically thin silicon film (filled circles). Curves result from theoretical calculations based on Auger heating (see text).

died. The results of this analysis at probe wavelength 485 nm and pump fluence 0.02 J/cm^2 are shown in Figs. 2(a) and 2(b). A wavelength as far in the blue as possible, consistent with good signal-to-noise ratio, was selected because the heating effect is largest and the plasma effect smallest in this part of the spectrum. The real index n [filled circles in Fig. 2(a)] drops immediately by 1.2% upon photoexcitation of an electron-hole plasma of initial density $5 \times 10^{20} \text{ cm}^{-3}$, determined independently by direct measurement of pump absorption. The value of n then rises as the lattice temperature rises and the plasma density decreases, primarily through Auger recombination; n returns to its original value at $\Delta t = 25 \text{ ps}$, then rises toward a final value nearly 1% higher than its initial value within 200 ps. By contrast, at infrared wavelengths, Δn never rose above zero in the time scale investigated, as shown by the data for probe wavelength $1.0 \mu\text{m}$ also plotted (circles) in Fig. 2(a). The large values of $\Delta n/n_0$ in these data have been scaled down by a factor of approximately 4 for direct comparison with the data of $\lambda = 0.485 \mu\text{m}$, as discussed in more detail below. Simultaneous with these changes in n , the changes in k shown in Fig. 2(b) were observed. A sharp spike $\Delta t = 0$ is observed which corresponds closely to the cross correlation of the excitation and probe pulses and probably results from sum-frequency absorption of a pump and probe photon. This is followed by a slowly decaying absorbance which

reaches a constant value after $\Delta t = 200$ ps, approximately 30% higher than the initial absorbance.

We now analyze the photoinduced index changes shown in Fig. 2 in terms of a simple model which includes plasma and lattice-heating effects. From the observed wavelength dependence of Δn at $\Delta t = 0$, and because the probing wavelength 485 nm lies well below the direct edge of silicon, we determined that the effect of the plasma on the refractive index at this wavelength is well described by a Drude model. At $\lambda = 1.0 \mu\text{m}$, the heat-induced index change is 3 times smaller than at $0.485 \mu\text{m}$,⁸ while the plasma-induced index change is more than 4 times greater. Thus, within our experimental error, the infrared data represent a pure plasma-induced index change and, when scaled by λ^2 , model the plasma-induced index change at 485 nm. To an excellent approximation, this fractional index change is given by

$$\Delta n/n_0 = -(2\pi e^2/\epsilon_0 m^* \omega^2) N, \quad (1)$$

where the silicon refractive index $n_0 = 4.3$ at 485 nm, dielectric constant $\epsilon_0 = 19$, and $m^* = 0.2m_e$ is the reduced effective mass for electrons and holes. The space-time evolution of the electron-hole pair density $N(x,t)$ is described by a one-dimensional continuity equation. In a film with thickness less than the optical absorption depth, however, diffusion is suppressed, so that Auger recombination dominates the temporal evolution of N according to the formula

$$dN/dt = -(C_e + C_h) N^3, \quad (2)$$

where C_e, C_h are the Auger coefficients for $e-e-h$ and $e-h-h$ processes, respectively. For carrier densities up to 10^{20} cm^{-3} these coefficients have been measured¹⁴ to be $C_e, C_h = (2.8, 0.99) \times 10^{-31} \text{ cm}^6 \text{ sec}^{-1}$. At higher densities, screening may reduce the Auger coefficients somewhat.¹⁵ As a first approximation, we neglect any density dependence of C_e, C_h , allowing analytic solution of (2). The simultaneous solution of Eqs. (1) and (2) yields an expression for the fractional plasma-induced index change at 485 nm, which can be used to fit the scaled infrared data in Fig. 2(a).

Lattice heating derives from two sources: (1) direct heating, caused by the emission of phonons by photoexcited carriers as they relax toward the band edge as far as allowed by the Pauli exclusion principle (this process occurs within a picosecond); (2) delayed Auger heating, caused by reheating of carriers by Auger recombination, which continues at a steadily decreasing rate for hundreds of picoseconds. Kurz and Bloembergen² have calculated that the temperature rise of a silicon surface excited by a 30-psec laser pulse is not completed for tens of picoseconds following the peak of the pulse. Because of the laser pulse width, however, direct experimental verification of this delay was not possible. To our knowledge the delayed posi-

tive index change shown in Fig. 2(a) is the first direct observation of delayed Auger heating. For a completely nondegenerate electron-hole plasma, no more than $(E_x - E_g)/E_x \approx 0.42$ of the excitation energy $E_x = 2.0$ eV can be lost by direct heating ($E_g = 1.15$ eV). As plasma degeneracy increases, the electron and hole quasi-Fermi levels approach the excess energy $E_x - E_g$, and Auger heating must increase in importance at the expense of direct heating. For a plasma density of 5×10^{20} , band filling reduces the fraction of the energy going to direct heating to less than 15% of the incident photon energy.¹⁶ The remainder must be lost by Auger heating. If we neglect carrier and heat diffusion on the time scale of interest, the Auger heating can be described by the simple energy-balance equation

$$\rho C_p dT/dt = (C_e + C_h) N^3 (E_g + kTH), \quad (3)$$

where H is a degeneracy factor equal to 3 for a nondegenerate plasma and increasing with degeneracy and carrier density. Although H strictly depends on density N , we can approximate H as a constant, thus allowing analytic solution of Eq. (3) using $N(t)$ as derived from the solution of Eq. (2). The temporal evolution of the positive fractional index change caused by Auger heating can be related to the temperature evolution by

$$\Delta n/n_0 = \beta \Delta T(t) n_0, \quad (4)$$

where $\beta = 8.0 \times 10^{-4} \text{ K}^{-1}$ at 485 nm.⁸

The lower dotted theoretical curve in Fig. 2(a) was obtained from simultaneous solution of Eqs. (1) and (2) with use of the measured initial density $N_0 = 5 \times 10^{20} \text{ cm}^{-3}$ and combined Auger coefficient $C_e + C_h = 3.0 \times 10^{-31} \text{ cm}^6 \text{ sec}^{-1}$. The upper theoretical curve was obtained by solution of Eqs. (3) and (4) with these same initial values. The middle curve, which fits the original data at 485 nm, is the sum of the upper and lower curves. The value of $C_e + C_h$ is somewhat lower than values measured at densities under 10^{20} cm^{-3} , indicating that some screening may be present. A small instantaneous fractional index change of +0.001 at $\Delta t = 0$ from direct heating was assumed. Clearly, this simple model satisfactorily explains the magnitude as well as the temporal evolution of the index changes shown in Fig. 2(a). At higher excitation fluences, we have observed that the index change rises considerably more rapidly. At a fluence of 0.06 J/cm^2 , $\Delta n/n_0$ crosses zero within 10 psec. This result is consistent with the faster Auger recombination and Auger heating rates expected at higher carrier densities, as described by the N^3 dependence shown in Eqs. (2) and (3).

The temporal evolution of the fractional change in k shown in Fig. 2(b) also appears to reflect the combined influence of plasma and lattice-heating effects.

The change in the imaginary index can be related to the temperature rise by the relation

$$\ln(k/k_0) = \Delta T/\theta, \quad (5)$$

where $\theta = 430$ K.⁸ The combined solution of Eqs. (3) and (5), which describes the effect of lattice heating on k , yields the dashed curve shown in Fig. 2 when the same initial conditions as above are assumed. Clearly, this curve deviates significantly from the data points at early times. The higher k values observed must arise from plasma-induced absorption, which probably results from excitation of the photoexcited electrons (holes) to higher- (lower-) energy conduction (valence) bands. Even though the electron-hole pair density is 2 orders of magnitude less than the valence-electron density, many of the inter-conduction- and inter-valence-band transitions are probably direct, thus explaining the large absorbance change observed. The temporal decay of the plasma-induced absorption results from Auger recombination of the photoexcited plasma. The dotted curve in Fig. 2 shows the linear plasma-induced absorbance $\sigma N(t)L$, with $\sigma = 1.6 \times 10^{-17}$ cm². This is about an order of magnitude larger cross section than that expected for free-carrier absorption.

More sophisticated calculations of the Auger heating process would take into account the density dependence of the degeneracy factor H and the Auger coefficients C_e, C_h and make use of numerical methods to solve Eqs. (1) through (5). We believe, however, that the simpler calculations outlined above capture the essential physics of the optical heating process in silicon. More detailed studies at higher excitation levels will be necessary to study the heating rate at the melting threshold, and thus to elucidate the relationship between heating rate and lattice disordering observed above E_{th} . Equations (3) and (5), obtained from measurements on samples in thermal equilibrium,⁸ appear to remain valid even on the short time scale involved in the present experiment. In metallic samples, only rapid direct heating would be expected.

We thank H. Kurz for several illuminating discussions.

^(a)Current address: Physics Department, The University of Texas at Austin, Austin, Texas 78712.

¹*Energy Beam-Solid Interactions and Transient Thermal Processing*, edited by J. C. C. Fan and N. M. Johnson, Materials Research Society Symposia Proceedings No. 23 (North-Holland, New York, 1984), and references cited therein.

²H. Kurz and N. Bloembergen, in *Energy Beam-Solid Interactions and Transient Thermal Processing*, Materials Research Society Symposia Proceedings No. 35 (Materials Research Society, Pittsburgh, 1985), and references cited therein.

³C. V. Shank, R. Yen, and C. Hirlimann, *Phys. Rev. Lett.* **50**, 454 (1983).

⁴C. V. Shank, R. Yen, and C. Hirlimann, *Phys. Rev. Lett.* **51**, 900 (1983).

⁵M. C. Downer, R. L. Fork, and C. V. Shank, *J. Opt. Soc. Am. B* **2**, 595 (1985).

⁶K. Murakami, K. Takita, and K. Masuda, *Jpn. J. Appl. Phys.* **20**, L867 (1981); K. Murakami, H. Itoh, K. Takita, and K. Masuda, *Physica (Amsterdam)* **117B**, 1024 (1983).

⁷L. A. Lompre, J. M. Liu, H. Kurz, and N. Bloembergen, *Appl. Phys. Lett.* **43**, 168 (1983).

⁸G. E. Jellison, Jr., and F. A. Modine, *Appl. Phys. Lett.* **41**, 180 (1982), and *J. Appl. Phys.* **53**, 3745 (1982), and *Phys. Rev. B* **27**, 7466 (1983), and Oak Ridge National Laboratory Report No. ORNL/TM-8002, 1982.

⁹P. B. Allen and M. Cardona, *Phys. Rev. B* **23**, 1495 (1981).

¹⁰O. S. Heavens, *Optical Properties of Thin Solid Films* (Dover, New York, 1985).

¹¹R. L. Fork, B. I. Greene, and C. V. Shank, *Appl. Phys. Lett.* **38**, 671 (1981).

¹²R. L. Fork, C. V. Shank, and R. Yen, *Appl. Phys. Lett.* **41**, 223 (1982).

¹³R. L. Fork, C. V. Shank, C. Hirlimann, R. Yen, and W. J. Tomlinson, *Opt. Lett.* **8**, 1 (1983).

¹⁴J. Dziewior and W. Schmid, *Appl. Phys. Lett.* **31**, 346 (1977).

¹⁵E. J. Yoffa, *Phys. Rev. B* **21**, 2415 (1980).

¹⁶J. R. Chelikowsky and M. I. Cohen, *Phys. Rev. B* **14**, 556 (1976).